Tensor Total-Variation Regularized Deconvolution for Efficient Low-Dose CT Perfusion

Ruogu Fang[1], Pina C. Sanelli[2,3], Shaoting Zhang[4], and Tsuhan Chen[1]

[1] Department of Electrical and Computer Engineering, Cornell University, Ithaca, NY
[2] Department of Radiology, Weill Cornell Medical College, New York, NY
[3] Department of Public Health, Weill Cornell Medical College, New York, NY
[4] Department of Computer Science, University of North Carolina at Charlotte, Charlotte, NC

Abstract. Acute brain diseases such as acute stroke and transit ischemic attacks are the leading causes of mortality and morbidity worldwide, responsible for 9% of total death every year. 'Time is brain' is a widely accepted concept in acute cerebrovascular disease treatment. Efficient and accurate computational framework for hemodynamic parameters estimation can save critical time for thrombolytic therapy. Meanwhile the high level of accumulated radiation dosage due to continuous image acquisition in CT perfusion (CTP) raised concerns on patient safety and public health. However, low-radiation will lead to increased noise and artifacts which require more sophisticated and time-consuming algorithms for robust estimation. We propose a novel efficient framework using tensor total-variation (TTV) regularization to achieve both high efficiency and accuracy in deconvolution for low-dose CTP. The method reduces the necessary radiation dose to only 8% of the original level and outperforms the state-of-art algorithms with estimation error reduced by 40%. It also corrects over-estimation of cerebral blood flow (CBF) and under-estimation of mean transit time (MTT), at both normal and reduced sampling rate. An efficient computational algorithm is proposed to find the solution with fast convergence.

1 Introduction

As the second leading cause of death worldwide, stroke is responsible for 4.4 million (9 percent) of the total 50.5 million deaths each year [1]. It affects more than 700,000 individuals annually in the United States (approximately one person every 45 seconds). It is also the No. 1 cause of disability among adults in US. Fast and accurate diagnosis and treatment for acute stroke is critical for the survival rate and life quality. Computed tomography perfusion (CTP) is the most widely used imaging modality for acute cerebrovascular disease diagnosis and detection, due to its widespread availability, rapid acquisition time, high spatial resolution and low cost. However, the elevated radiation dosage issue has raised significant public concerns regarding its potential biological effects, such as hair loss, skin damage, cataract formation, very small but definite increase of cancer risk [2].

The low-dose protocols, on the other hand, are leading to higher photon and imaging noise, which is compensated by more complicated and time-consuming algorithms with spatial smoothing, reduced matrix reconstruction and/or thick-slices, with the cost

P. Golland et al. (Eds.): MICCAI 2014, Part I, LNCS 8673, pp. 154–161, 2014.

of longer processing time, lowering spatial resolution and accuracy [3, 4]. While edge-preserving filtering algorithms are relatively slow in computation, HighlY constrained back-PRojection (HYPR) and Markov Random Fields (MRF) require motion-free images across the scan duration. Furthermore, these algorithms attempt to reduce the noise in the reconstructed CT image series, instead of improving the deconvolution process or the quantification of perfusion maps.

In this work, we propose an efficient and accurate deconvolution algorithm to improve the perfusion parameter estimation at low dose by tensor total variation (TTV) regularized deconvolution. All the previously mentioned noise reduction algorithms for CT image sequences can complement our model to further reduce the noise and improve the image quality. Total variation has been proposed for low-dose CT image reconstruction [5], while here we address a different problem of deconvolution to estimate the perfusion parameters.

The contribution of our work is three-fold. First, we propose to regularize the impulse residue functions instead of the perfusion parameter maps. Second, the optimization is performed globally on the entire spatio-temporal data, instead of each patch individually. Third, total variation regularizer is extended into the three dimensional sequence to consider the regional effect and temporal correlation of the tissue. The method reduces the necessary radiation dose to only 8% of the original level and outperforms the state-of-art algorithms with estimation error reduced by 40%. It also corrects over-estimation of cerebral blood flow (CBF) and under-estimation of mean transit time (MTT), at both normal and reduced sampling rate. An efficient computational algorithm is proposed to find the solution with fast convergence.

2 Tensor Total Variation Regularized Deconvolution

2.1 CT Perfusion Convolution Model

The physiological model of blood flow in CTP is built on tracing the intravenously injected contrast agent using X-ray scans. For a volume under consideration V_{voi}, let AIF (arterial input function) be the contrast agent concentration at the artery inlet, and C_{voi} be the average contrast agent concentration in V_{voi}. ρ_{voi} is the mean density of the volume V_{voi}. The residue function $R(t)$ quantifies the relative amount of contrast agent that is still inside the volume V_{voi} of interest at time t after a contrast agent bolus has entered the volume at the arterial inlet at time $t = 0$.

CBF is defined as the blood volume flow normalized by the mass of the volume V_{voi} and is typically measured in mL/100g/min. MTT, usually measured in seconds, is defined as the first moment of the probability density function $h(t)$ of the transit times.

The convolution model can be expressed as follows:

$$C_{voi}(t) = (AIF \otimes K)(t) \tag{1}$$

where the flow-scaled residue function $K(t)$ is introduced:

$$K(t) = CBF \cdot \rho_{voi} \cdot R(t) \tag{2}$$

By forming the matrix-vector notation, the convolution can be formulated as matrix multiplication. For a volume of interest with N voxels, we have

$$C = AK \tag{3}$$

where $C = [c_1, \ldots, c_N] \in \mathbb{R}^{T \times N}$, $K = [k_1, \ldots, k_N] \in \mathbb{R}^{T \times N}$ represent the contrast agent concentration and scaled residue function for the N voxels in the volume of interest. To overcome the inaccuracies due to delay and dispersion of the contrast agent, block-circulant version of A and C are adopted [6] to make the algorithm insensitive to the tracer arrival time. The perfusion parameters CBF and MTT can be determined from K [7].

2.2 Tensor Total Variation Regularized Deconvolution

The least square solution of Eq. (3) is equivalent to minimizing the squared Euclidean residual norm of the linear system given by Eq. (3) as

$$K_{ls} = \underset{K \in \mathbb{R}^{T \times N}}{\arg\min} (\|AK - C\|_2^2) \tag{4}$$

However, for the ill-conditioned Toeplitz matrix A, the least-square solution K_{ls} does not represent a proper solution. A small change in C (e.g. due to projection noise or low-dose scan) can cause a large change in K_{ls}. Regularization is necessary to avoid the strong oscillation in the solution due to small singular values of matrix A.

Since the voxel dimensions in a typical CTP image are much smaller than tissue structures, changes in perfusion are regional effects rather than single voxel effects. Our assumption is that within extended voxel neighborhoods the perfusion parameters will be constant or of low-variation. Meanwhile, it is also important to identify edges between different regions where tissues undergo perfusion changes, particularly ischemic regions. In the temporal dimensional, the residue functions are continuous, while the rapid rise and slow decay of contrast agent should also be preserved. We introduce the tensor total variation regularizer to the data fidelity term in Eq. (4) as

$$K = \underset{K \in \mathbb{R}^{T \times N}}{\arg\min} (\frac{1}{2}\|AK - C\|_2^2 + \gamma \|K\|_{TV}) \tag{5}$$

where γ is a positive parameter. It is based on the assumption that the piecewise smooth residue functions in CTP should have small total variation in both the temporal and spatial domain. Here we use a same $\gamma = 1$ for the spatial and temporal dimension, which yields satisfactory results. The tensor total variation term is defined as

$$\begin{aligned} \|K\|_{TV} = \sum_{t,i,j,k} (&|\tilde{K}_{t+1,i,j,k} - \tilde{K}_{t,i,j,k}| + |\tilde{K}_{t,i+1,j,k} - \tilde{K}_{t,i,j,k}| \\ &+ |\tilde{K}_{t,i,j+1,k} - \tilde{K}_{t,i,j,k}| + |\tilde{K}_{t,i,j,k+1} - \tilde{K}_{t,i,j,k}|) \end{aligned} \tag{6}$$

where $\tilde{K} \in \mathbb{R}^{T \times N_1 \times N_2 \times N_3}$ is the 4-D volume obtained by reshaping matrix K based on the spatial and temporal dimensions. Here $N = N_1 \times N_2 \times N_3$ and T is the time

Algorithm 1. The framework of TTV algorithm.

Input: Regularization parameters γ
Output: Flow-scaled residue functions $K \in \mathbf{R}^{T\times N_1\times N_2\times N_3}$.
$K^0 = 0$
$t^1 = r^1 = K^0$
for $n = 1, 2, \ldots, N$ **do**
(1) Steepest gradient descent: $K_g = r^n + s^{n+1}(A^T(C - Ar^n))$
where $s^{n+1} = \frac{Q^TQ}{(AQ^T)(AQ)},\ Q \equiv A^T(Ar^n - C)$
(2) Proximal map: $K^n = prox_\gamma(2\|K\|_{TV})(K_g)$,
where $prox_\rho(g)(x) := \arg\min_u \left\{ g(u) + \frac{1}{2\rho}\|u - x\|^2 \right\}$
(3) Update t, r: $t^{n+1} = (1+\sqrt{1 + 4(t^n)^2})/2, r^{n+1} = K^n+((t^n-1)/t^{n+1})(K^n-K^{n-1})$
end for

duration. The tensor total variation term here uses the forward finite difference operator with L_1 norm. The regularization parameter γ controls the regularization strength, and the larger the γ, the more smoothed the residue functions. Since the TV term is non-smooth, this problem is difficult to solve. Conjugate gradient (CG) and partial differential equation (PDE) methods could be used to attack it, but they are very slow and impractical for real CTP images. Motivated by the effective acceleration scheme in Fast Iterative Shrinkage-Thresholding Algorithm (FISTA) [8, 9], we propose a total variation regularization algorithm (Algorithm 1) to efficiently solve the problem in Eq. (5). We extended the 2-dimensional TV regularizer in [8] to 4-dimensional and adapted the algorithm to tensor total variation, to impose both temporal and spatial edge-preserving regularization.

2.3 Implementation Details

All algorithms were implemented using MATLAB 2013a (MathWorks Inc, Natick, MA) on a MacBook Pro with Intel Core i7 2.8G Hz Duo CPU and 8GB RAM. Four baseline methods were compared: standard truncated singular value decomposition (sSVD) [7], block-circulant truncated SVD (bSVD) [6], Tikhonov regularization (Tikh) [10] and sparse perfusion deconvolution (SPD)[11]. Perfusion maps are computed on the high-dose 190 mA and the simulated low-dose 15 mA images by adding correlated statistical noise [12] with standard deviation of $\sigma_a = 25.54$, which yields PSNR=40. The maps calculated using bSVD from the 190 mA high-dose CTP data is regarded as the "gold standard" or reference images in clinical experiments. A threshold value λ is empirically chosen as 0.1 (10% of the maximum singular value) to yield optimal performance for SVD-based algorithms. One-tail student test is used to determine whether there is significant difference between the evaluation metrics of the comparing algorithms. A α level of .05 is used for all statistical tests to indicate significance. Two metrics were used to evaluate the image fidelity to the reference: Root mean-squared-error (RMSE) and Lin's Concordance Correlation Coefficient (CCC). Low RMSE and high Lin's CCC indicate high accuracy for the perfusion maps.

3 Experiments

3.1 Synthetic Studies

Because the clinical CTP does not have ground truth perfusion parameter values for comparison, we first use synthetic data to evaluate the proposed algorithm, following the synthetic experiment setup in [13].

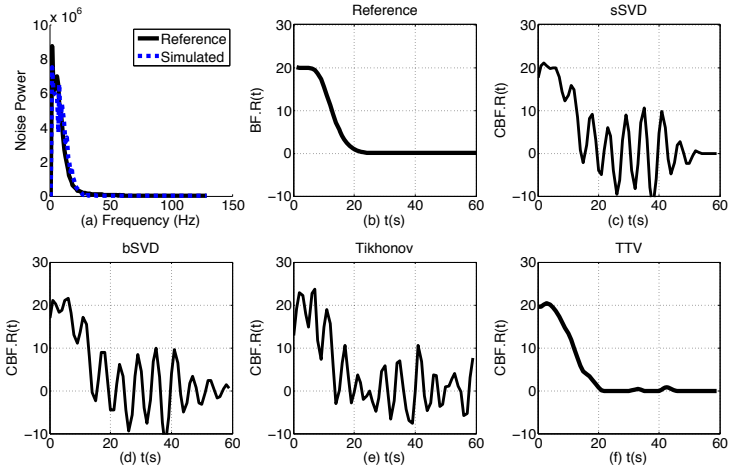

Fig. 1. The Noise power spectrum and the recovered residue functions by baseline methods and TTV. (a) The noise power spectrum is of the scanned phantom image at 15 mA and simulated statistical correlated Gaussian noise at 15 mA. (b)-(f) The parameters used for residue function recovery are the simulation is CBV = 4 mL/100 g, CBF = 20 mL/100 g/min, PSNR=25. SPD is not included since it optimizes the perfusion maps directly.

Residue Recovery: The simulated noise power spectrum (NPS) at 15 mA is compared with the NPS of the real scanned phantom image at 15 mA, as shown in Figure 1(a). The residue function recovered by the baseline methods and TTV are shown in Figure 1(b-f). The baseline methods show severe oscillation and elevated peak value, while the residue function recovered by TTV is in agreement with the reference.

Uniform Region Estimation: From the recovered residue function, perfusion parameters CBF and MTT can be estimated. We generate a small region containing 40×40 voxels with the same perfusion characteristics, and compute the mean and standard deviation of the perfusion parameters over this region. 1) Fig. 2 (a)-(b) show the estimated CBF and MTT values when the true perfusion parameter values vary. All the baseline methods overestimate the CBF values and under-estimate the MTT values while TTV yields accurate CBF and MTT estimations. 2) To explore the effect of noise levels on the performance of perfusion parameter estimation, we simulate different levels of noise (PSNR varies from 5 to 60) and fix CBF at 20 mL/100 g/min and MTT at 12 s. Fig. 2 (c)-(d) show the estimation results. When the accuracy of the baseline methods degrades

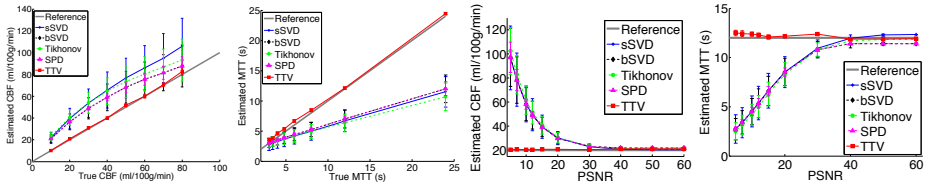

Fig. 2. Comparison of the accuracy in estimating CBF and MTT by sSVD, bSVD, Tikhonov, SPD and TTV deconvolution methods. True CBV = 4 mL/100 g. The error bar denotes the standard deviation. (a) Estimated CBF values at different true with PSNR=15. (b) Estimated MTT values at different true MTT with PNSR=15. (c) Estimated CBF values at different PSNRs with true CBF=20 mL/100 g/min. (d) Estimated MTT values at different PSNRs with true MTT = 12 s.

Table 1. Quantitative evaluation of the perfusion parameters in Fig. 2. 'Estimated' mean the perfusion parameter to be estimated. 'Condition' means the varying condition. The best performance is highlighted in bold font.

Estimated	CBF			MTT		
Varying	CBF		PSNR	MTT		PSNR
Method/Metric	RMSE	Lin's CCC	RMSE	RMSE	Lin's CCC	RMSE
sSVD	23.52	0.6878	52.07	6.056	0.4283	6.278
bSVD	15.05	0.8129	52.01	5.827	0.4567	6.309
Tikhonov	19.94	0.7198	43.92	5.64	0.4748	6.015
SPD	15.02	0.8294	44.36	5.804	0.4586	3.3323
TTV	**0.993**	**0.9991**	**0.7954**	**0.6847**	**0.9945**	**0.294**

Table 2. Quantitative comparison of five methods on ten patients in terms of RMSE, Lin's CCC and linear regression. The best performance is highlighted in bold font. * $P < .001$ in one-tail student test compared to the four baseline methods.

Method	RMSE	Lin's CCC
sSVD	25.69	0.049
bSVD	7.60	0.185
Tikhonov	11.27	0.161
SPD	6.03	0.267
TTV	**3.63***	**0.505***

dramatically as the noise level increases, TTV method appears to be more robust. Table 1 shows the quantitative evaluation of the different methods in terms of RMSE and Lin's CCC while the ground truth parameter or the PSNR varies.

3.2 Clinical Studies

Retrospective review of consecutive CTP exams performed on aneurysmal subarachnoid hemorrhage patients enrolled in an IRB-approved and HIPAA-compliant clinical trial from August 2007-July 2013 was used. Ten consecutive patients (9 women, 1 men) admitted to the Weill Cornell Medical College, with mean age (range) of 54 (35-83) years were included. 5 patients had brain deficits shown in the CTP images and the other 5 patients had normal brain images.

Visual Comparison: At normal sampling rate, Fig. 3 shows significant differences visually between the CBF maps of the different deconvolution methods, where sSVD, bSVD, Tikhonov and SPD overestimate CBF, while TTV estimates accurately. At reduced temporal sampling rate by downsampling 2 times, the errors in the four baseline methods increase, while TTV maintains accurate estimation, with the potential to further minimize the radiation dosage level by increasing sampling intervals.

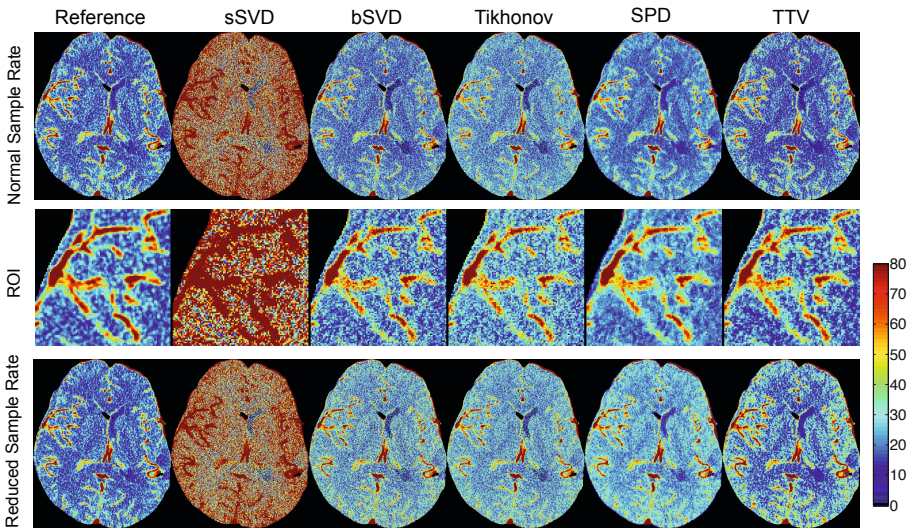

Fig. 3. The CBF maps with zoomed ROI regions of a patients calculated using different methods at normal sampling rate (first two rows) and reduced rate by downsampling 2 times (bottom row). Baseline methods sSVD, bSVD and Tikhonov overestimate CBF values, while SPD and TTV correspond with the reference. At reduced rate, the difference is more significant. (Color image)

Quantitative Comparison: There is significant improvement in image fidelity between the low-dose CBF maps and the high-dose CBF maps by using the TTV algorithm compared to the baseline methods. On average, the RMSE decreases by 40%, Lin's CCC increases by 89% from the best performance by using the baseline methods (Table 2).

Computation Time: It takes approximately 25 s to process a clinical dataset of $512 \times 512 \times 118$ by TTV method with 5 iterations, and approximately 0.83 s, 2.04 s and 1.35 s for sSVD, bSVD and Tikhonov algorithms. For SPD, it takes 80.6 s for the whole image. The TTV algorithm usually converges within 5 iterations. Though SVD and Tikhonov based methods are faster, the over-estimation, low spatial resolution, less differentiable tissue types and graining in the image in the perfusion maps generated by these baseline methods for the low-dose data are not acceptable. SPD reduces the variation in the smooth region to certain extent, however, TTV takes only 30% of the computation time compared to the time for SPD and yields more accurate estimation.

4 Conclusion

In this study, a new tensor total variation regularized deconvolution algorithm is proposed to improve the quality and quantification of the low-dose CTP perfusion maps and extensively compared with the existing widely used algorithms, e.g. sSVD, bSVD and Tikhonov regularization, as well as SPD for low-dose deconvolution. Synthetic evaluation with accurate ground truth data is used to compare the quality of the residue functions, uniform regions, sensitivity to hemodynamic conditions and noise levels. Clinical

evaluation using high-dose perfusion maps as the reference image is conducted to show the visual quality and data fidelity at normal and reduced sampling rate. The proposed TTV method is able to achieve both high accuracy and computational efficiency to save critical time for the clinical diagnosis.

References

[1] Feigin, V.L., Lawes, C.M., Bennett, D.A., Barker-Collo, S.L., Parag, V.: Worldwide stroke incidence and early case fatality reported in 56 population-based studies: a systematic review. The Lancet Neurology 8(4), 355–369 (2009)

[2] Wintermark, M., Lev, M.: FDA investigates the safety of brain perfusion CT. American Journal of Neuroradiology 31(1), 2–3 (2010)

[3] Saito, N., Kudo, K., Sasaki, T., Uesugi, M., Koshino, K., Miyamoto, M., Suzuki, S.: Realization of reliable cerebral-blood-flow maps from low-dose CT perfusion images by statistical noise reduction using nonlinear diffusion filtering. Radiological Physics and Technology 1(1), 62–74 (2008)

[4] Supanich, M., Tao, Y., Nett, B., Pulfer, K., Hsieh, J., Turski, P., Mistretta, C., Rowley, H., Chen, G.H.: Radiation dose reduction in time-resolved CT angiography using highly constrained back projection reconstruction. Physics in Medicine and Biology 54(14), 4575 (2009)

[5] Tian, Z., Jia, X., Yuan, K., Pan, T., Jiang, S.B.: Low-dose ct reconstruction via edge-preserving total variation regularization. Physics in Medicine and Biology 56(18), 5949 (2011)

[6] Wu, O., Østergaard, L., Weisskoff, R.M., Benner, T., Rosen, B.R., Sorensen, A.G.: Tracer arrival timing-insensitive technique for estimating flow in MR perfusion-weighted imaging using singular value decomposition with a block-circulant deconvolution matrix. Magnetic Resonance in Medicine 50(1), 164–174 (2003)

[7] Østergaard, L., Weisskoff, R.M., Chesler, D.A., Gyldensted, C., Rosen, B.R.: High resolution measurement of cerebral blood flow using intravascular tracer bolus passages. Part I: Mathematical approach and statistical analysis. Magnetic Resonance in Medicine 36(5), 715–725 (1996)

[8] Beck, A., Teboulle, M.: A fast iterative shrinkage-thresholding algorithm with application to wavelet-based image deblurring. In: IEEE International Conference on Acoustics, Speech and Signal Processing, ICASSP 2009, pp. 693–696. IEEE (2009)

[9] Huang, J., Zhang, S., Metaxas, D.: Efficient MR image reconstruction for compressed MR imaging. Medical Image Analysis 15(5), 670–679 (2011)

[10] Fieselmann, A., Kowarschik, M., Ganguly, A., Hornegger, J., Fahrig, R.: Deconvolution-based CT and MR brain perfusion measurement: theoretical model revisited and practical implementation details. Journal of Biomedical Imaging 2011, 14 (2011)

[11] Fang, R., Chen, T., Sanelli, P.C.: Towards robust deconvolution of low-dose perfusion ct: Sparse perfusion deconvolution using online dictionary learning. Medical Image Analysis 17(4), 417–428 (2013)

[12] Britten, A., Crotty, M., Kiremidjian, H., Grundy, A., Adam, E.: The addition of computer simulated noise to investigate radiation dose and image quality in images with spatial correlation of statistical noise: an example application to x-ray ct of the brain. British Journal of Radiology 77(916), 323–328 (2004)

[13] He, L., Orten, B., Do, S., Karl, W.C., Kambadakone, A., Sahani, D.V., Pien, H.: A spatio-temporal deconvolution method to improve perfusion ct quantification. IEEE Transactions on Medical Imaging 29(5), 1182–1191 (2010)